GEOMETRIC CALIBRATION OF THE STEREOSCOPIC CCD-LINESCANNER MOMS-2P

W. Kornus [1], M. Lehner [1], F. Blechinger [2], E. Putz [3]

[1] German Aerospace Research Establishment (DLR), Institute of Optoelectronics, Optical Remote Sensing Division
D-82230 Wessling, Germany; e-mail: wk@oe.op.dlr.de, manfred@oe.op.dlr.de

[2] Daimler-Benz Aerospace AG (Dasa), Dornier Satellitensysteme
D-81663 Munich, Germany; e-mail: 100347.3010@compuserve.com

[3] Technical University Munich, Chair for Photogrammetry and Remote Sensing
D-80290 Munich, Germany; e-mail: putz@photo.verm.tu-muenchen.de

Commision I, Working Group 3

KEY WORDS: Calibration, Scanner, Accuracy, Matching, Simulation, Geometric Scanner Calibration, Multi Scale Matching, MOMS-2P/PRIRODA Mission

ABSTRACT

This paper describes the geometric calibration of the **M***odular* **O***ptoelectronic* **M***ultispectral* **S***canner* MOMS-2P, which will collect threefold stereoscopic panchromatic and multispectral imagery of the earth with 18 m and 6 m ground pixel size from the PRIRODA module of the Russian space station MIR. The goal of the geometric calibration is the knowledge of the exact object side image angles for a precise photogrammetric three-dimensional reconstruction of the earth's surface, considering all geometric influences of the scanner like irregularities of the CCD-arrays, bending and relaxation of the focal plates, distortion of the optics, etc. Prior to the mission the optical system has been calibrated in the laboratory of *Daimler-Benz Aerospace AG* (Dasa), which is also the developer and manufacturer of the scanner. During the mission a geometric inflight calibration will be performed in order to verify the calibration parameters on a routine basis. The first part of the paper describes the lab-calibration, the equipment, the process and shows also the resulting calibration parameters. The second part deals with the inflight calibration. The principle, the test areas and the mission scenario are outlined. An approach for multi-scale matching using line scanner imagery and existing digital orthoimages is described. Finally the results of a simulation study are presented, showing to which extend the camera parameters can be determined by photogrammetric means under realistic conditions.

1 INTRODUCTION

During the 10 day lasting D2 mission in spring 1993 the first threefold along track stereoscopic imagery were recorded from space by MOMS-02 [11]. A series of photogrammetric evaluations were published, demonstrating its capability of generating photogrammetric products like digital terrain models (DTM) with an accuracy of 10 meters and less (e.g. [1], [5], [6], [8], [10]). After D2, MOMS-02 has been refurbished and adapted to the PRIRODA environment for a refly on-board the Russian space station MIR. Besides the now called MOMS-2P, the PRIRODA (*Russian: nature*) module contains a series of remote sensing sensors (see Figure 1) and will be docked on the MIR-station by mid April 1996. MOMS-2P consists of 5 lenses for simultaneous multispectral and panchromatic 3-fold stereoscopic data acquisition with a ground resolution of 18 m and 6 m from approximately 400 km height (see Figure 2). The stereo module consists of 3 lenses with one CCD-array each, providing a forward, a high resolution nadir and an aft looking view. Additional 2 lenses with 2 CCD-arrays each enable multispectral imaging in 4 spectral channels. The MOMS-2P/PRIRODA mission will last at least 18 months and can be considered as preparation for a future operational and commercial MOMS-03 mission, planned for the end of this decade. The operational derivation of DTM and digital orthoimages (DOI) of wide parts of the solid earth's surface is a major goal of both missions.

The photogrammetric evaluation is based on a measurement technique using intersecting spatial image rays, whose locations are defined by two image angles around two orthogonal axes with respect to the optical axis of a camera or a scanner system. By means of a camera model, these angles normally are expressed in terms of image coordinates. For the precise transformation of image coordinates into spatial image angles, the camera model must accurately represent the actual camera geometry implying its perfect knowledge. Since image coordinates are derived by digital measurement techniques with up to 0.1 pixel precision, the accuracy of the geometric camera calibration must not exceed this value, if the overall accuracy potential shall not be restricted by the system itself. In order to meet this requirement the process of the geometric camera calibration has been split into two parts: a laboratory (lab-)calibration prior to the mission and an inflight calibration accompanying the whole mission. The inflight calibration is of highest importance, since the results of the lab-calibration proved to be reproducible in some cases only up to 0.5 pixel accuracy. Furthermore, temporal changes of the camera geometry appeared in the MOMS-02/D2 evaluations indicating, that the lab-measurements may not exactly match the actual camera geometry in space.

The main goal of the lab-calibration is the exact determination of geometric irregularities of the single CCD-arrays, which hardly can be determined by inflight methods. The inflight calibration is for the verification or change detection of the camera parameters and to determine the orientation of the MOMS-2P camera axes with respect to the MIR coordinate system in order to improve the knowledge about the

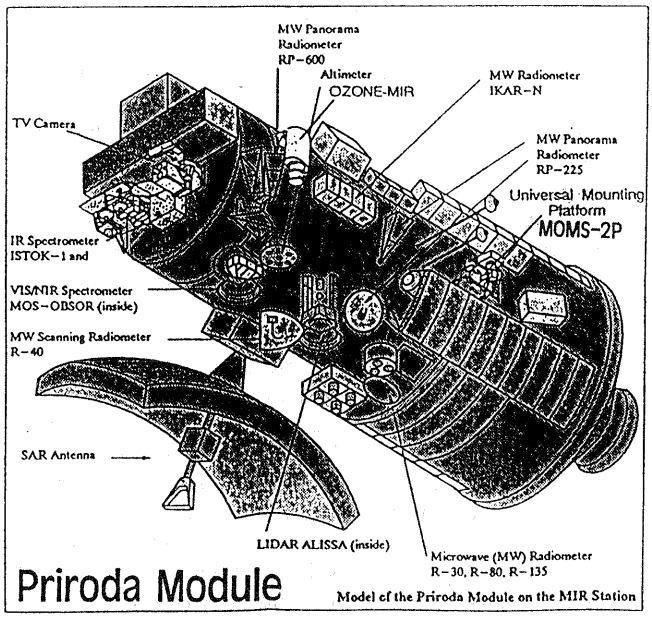

Figure 1: PRIRODA module on the MIR station

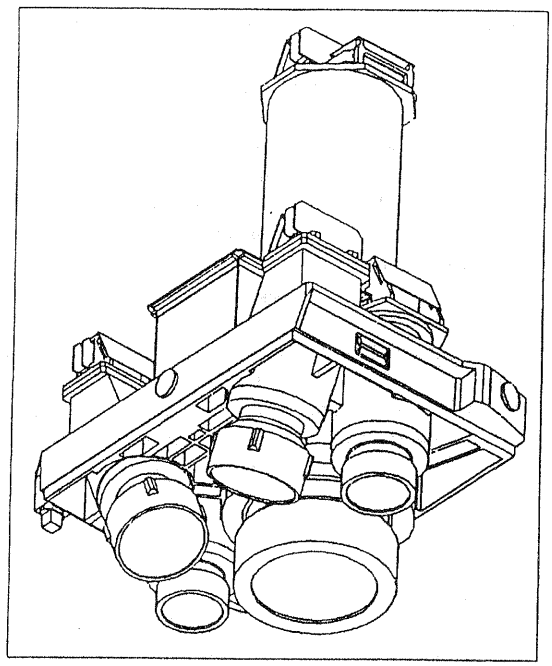

Figure 2: Optics module of MOMS-2P

absolute pointing of MOMS-2P. These investigations will also try to include the star camera on MIR module Quant.

This paper is organized in two main sections and a final conclusion part. The following section describes the lab-calibration, the equipment, the process and shows the resulting calibration parameters. The next section deals with the inflight calibration. The principle, the test areas and the mission scenario are outlined. A technique for the automated identification of a large number of ground control points, via an approach for multi-scale matching using line imagery and existing DOI is described. Subsequently, the results of a simulation study are presented, showing to which extend the camera parameters can be determined by photogrammetric means under realistic conditions.

2 LAB-CALIBRATION

Extensive alignments and measurements have been performed in the laboratory to characterize the MOMS-2P optics module. The main tasks were:

- Alignment of the CCD detectors into the optimum focal plane of each lens assembly. Since the lenses are nearly diffraction limited (i.e. the physical limit), the tolerance for focus adjustment was < 20 μm.
- Lateral adjustment to obtain exact superposition of all detector arrays. The ground footprints of all CCD-arrays (i.e. the geometrical projection of the CCD's through the lenses onto the earth surface) shall be correlated with sub-pixel accuracy (< 0.1 pixel) which corresponds to alignment and stability tolerances of 1 μm at detector level.
- Adjustment of the projected image size between all channels, which implies that the focal length of all five lenses must be matched with sub-pixel accuracy. Note that the relative focal length accuracy is $3 \cdot 10^{-5}$.
- Measurements of detector geometry and the relation of the individual channels together, again with sub-pixel accuracy.
- Relative and absolute radiometric calibration.

An important aspect for all on-ground testing activities was the fact that the instrument shall be characterized for vacuum conditions. The optics module, however, exhibits significantly different performances when operated in vacuum or in air. This effect is due to the small but finite refractive index difference between air ($n_e = 1.000297$) and vacuum ($n_e = 1.000000$). A natural approach to cope with this problem would be to place the entire optics module and all associated test equipment in a vacuum chamber. However, the drawbacks would be very inconvenient such that there is no direct access to the equipment and to adjustment tools other than by remote (computer) control, that the required facilities are very expensive and that the resulting logistic difficulties would stretch the time scale extremely.

The dedicated solution for MOMS-2P was found in air spaced doublets which are used only for ground testing. For each lens assembly an individual doublet was designed and manufactured. Attached to the lens assembly, the doublets exactly compensate the change of focal length and of focus position when going from air to vacuum. This approach was the prerequisite to predict and characterize the overall system performance for vacuum conditions.

2.1 Calibration Procedure

The calibration procedure was based on the philosophy to design the test setup for maximum commonality, i.e. to reduce the number of dedicated equipment and to reduce the number of required changes of the test setup for individual measurements. Basically, the test setup for MOMS-2P has been dictated by the very high geometric accuracy requirements. For this reason, all channels (and therefore all lens assemblies) were stimulated simultaneously by the same source.

Typically, a pinhole in the focal plane of a large aperture and long focal length collimator served as an artificial star. The star intensity and its spectral distribution was adjustable by appropriate filters in the illumination optics. The emerging light from the collimator is a plane wavefront illuminating in parallel all entrance apertures of the MOMS-2P optics module. Each lens forms an image of the artificial star on the CCD-arrays in the corresponding focal planes. By direct read-out of the CCD-response using the nominal signal processing electronics, an end-to-end performance of the system is obtained. Therefore, this approach takes into account all possible sources of deterioration in the entire chain, namely the residual aberrations of the optics, the focus and alignment condition, the detector response and detector internal cross-talk, and finally the quantization and noise effects of the signal processing electronics. The principle test setup which is used for all subsequent measurements is given in Figure 3.

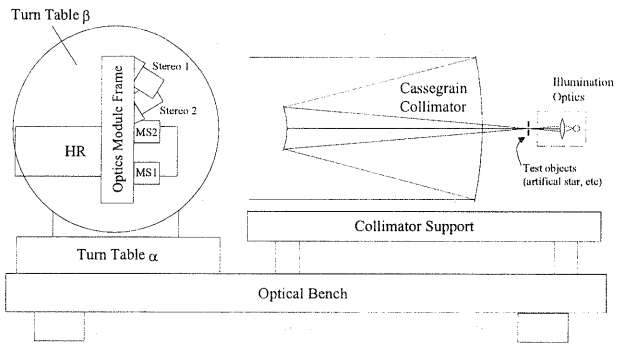

Figure 3: Principle test setup for calibration of MOMS-2P optics module

Geometrical Alignment And Calibration: The geometrical correlation is obtained by measuring the gravity center of the star image intensity distribution in relation to a precisely known angle in the object space of the sensor. Assuming a distortion free optics (which has been ensured by the theoretical design and high precision manufacturing and assembling at the manufacturer), the relation between a position x, y at the CCD and the corresponding object angles α, β is:

$$\tan(\alpha) = \frac{x}{FL} \quad \text{and} \quad \tan(\beta) = \frac{y}{FL} \qquad (1)$$

with:

FL	=	Focal Length of the system, including detector
x, y	=	Coordinates at detector
α, β	=	Angles in object space

Thus, if the optics module is stimulated at a certain angle α, β, the deviation of the measured spot image gravity center from the nominal position x, y can be obtained. Inversely, if a large number of data pairs x, y vs. α, β is measured, an average value for the system focal length FL can be deduced, which is listed in Table 1 for each channel. FL shall be identical for all channels respectively in a defined relationship to each other (i.e. relation 1:3 between the nadir high resolution (HR) stereo channel and the other channels).

For the geometric measurements, the gravity center of the star image has been centered on about 15 pixels per CCD-array in an approximate 400 pixel interval. For these pixels the x, y, α, β data set has been recorded. To increase the measurement accuracy and to eliminate systematic errors caused by the turn table axis geometry, four data sets per CCD-array have been recorded. Data sets 1 and 3 were measured in normal position, data sets 2 and 4 in reverse position, i.e. MOMS-2P is rotated 180° around both the horizontal and the vertical turn table axis. The mean value of the measure in normal and reverse position is free of systematic errors, e.g. the deviation of horizontal and vertical turn table axis from 90° (see section 2.3). Thus, the geometry of each CCD-array is defined by 15 data points times 4 data sets = 60 data points. This "raw" data set has been further refined by interpolation into a finer equidistantly spaced interval of 200 pixels per sensor. Special precautions on the selection of the appropriate interpolation algorithm were necessary to preserve the shape of the data set and to avoid "overshooting" effects at the upper and lower limits of the sensor. After several tests, the Akima interpolation turned out to be the optimum without deteriorating the raw data by more than 0.1 pixel. Note: The interpolation can be avoided by directly measuring a 200 pixel interval. However, the measurement of a single pixel to the desired sub-pixel accuracy is a time consuming process involving many iteration steps in the turn table control. Although the measurement process was automated by computer, a single CCD-array measurement (15 data points) lasted several hours. Thus, simply to achieve an economic calibration procedure, the 400 pixel interval with subsequent interpolation was decided.

2.2 Calibration Equipment

In order to fulfill the alignment and calibration task, the on-ground equipment has been specifically designed with the following performance figures:

Collimator The collimator is an on-axis "Cassegrain" telescope inversely used. It provides a usable aperture of 650 mm to illuminate all lenses simultaneously. The focal length is 7.8 m which allows relatively large dimensions for the object structures (pinhole diameter) and thus, reduces tolerances. The wavefront quality over the full aperture is better $\lambda/8$ peak to valley. Taking into account that each lens of the MOMS-2P optics module uses only a small fraction of the full aperture, the residual measurement error introduced by the collimator is $< \frac{1}{70}$ of a pixel which is negligible compared to other error sources in the test setup.

A crucial point is the perfect collimation (i.e. the artificial star is virtually at infinity), since it determines then the final resolution (modulation transfer function, MTF) of the overall system. The "infinity" condition of the test equipment is referred to a precision flat of same size as the collimator aperture and two independent focusing principles ("Knife Edge" test and Point Spread Function PSF in autocollimation). This approach has been selected to avoid systematic errors (Hubble effect!).

Angular Reference (Two-Axis Turn Table) The angular reference to obtain the object angles α, β is provided by a high precision two-axis turn table with precision encoders (Heidenhain ROD 800). The minimum resolvable angle is 0.36", accounting to 1/7 pixel measurement error of the HR CCD-array. This is probably the worst figure in the overall error budget, but it must be noted that this encoder accuracy was the best available on the market at the time of the design of the instrument and the test facilities.

Optical Benches In view of the required verification accuracies (sub-arcsec), the entire test setup (collimator, turn table, MOMS-2P instrument) was mounted on a single rigid optical bench with air pressurized support and on a concrete solid block being entirely separated from the rest of the building The entire integration / test facility was operated in controlled clean room environment (class < 100000), and controlled temperature and humidity.

Dedicated Software (Sub-Pixel Interpolation) A dedicated software has been written to interface the test equipment with the MOMS-2P signal processing electronics, to control the turn table position, to acquire the precise angular readings and to compute the gravity center of the point spread functions imaged at the CCD's.

2.3 Results

From the four data sets camera parameters and correction tables were deduced. The camera parameters (see Table 1) describe the locations of the CCD-arrays relative to each other, the correction Tables 2 and 3 show the differences between the actual and the nominal position of the sensor elements. The positions are given with respect to a reference pixel coordinate system, defined in the (object side) image plane at a distance of the mean focal length FL from the projection center. Its origin is at the center of pixel number 4501 of the high resolution CCD-array HR5A. The positive y-axis is pointing in flight direction, the positive x-axis along line in the direction of decreasing pixel numbers (see Figure 4). Table 1 contains

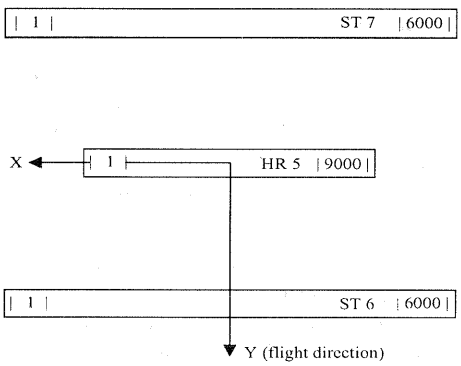

Figure 4: Reference pixel coordinate system

the mean focal length FL, the offset pixel numbers N_{Xoff} and the stereo angles γ for each channel. N_{Xoff} indicates at which pixel number the y-axis intersects the CCD-array.

Channel	FL [mm]	N_{Xoff}	γ [°]
MS1	220.163	3006.0	0.00
MS2	220.096	3008.0	0.00
MS3	220.116	3016.8	0.00
MS4	220.088	3016.2	0.00
HR5	660.250	4500.5	0.00
ST6	237.241	3009.0	21.45
ST7	237.250	3020.1	-21.45

Table 1: Calibrated camera parameters

In the Tables 2 and 3 the differences $\begin{Bmatrix} dx \\ dy \end{Bmatrix} = \begin{Bmatrix} x_{CAL} - x_{NOM} \\ y_{CAL} - y_{NOM} \end{Bmatrix}$ between the calibrated and the nominal pixel positions are listed. $\begin{Bmatrix} x_{CAL} \\ y_{CAL} \end{Bmatrix}$ and $\begin{Bmatrix} x_{NOM} \\ y_{NOM} \end{Bmatrix}$ are derived for each calibrated pixel N according to equations 4 and 5:

$$\begin{Bmatrix} x_I \\ y_I \end{Bmatrix} = \frac{1}{2} \begin{Bmatrix} x_{set1} + x_{set2} \\ y_{set1} + y_{set2} \end{Bmatrix} \quad (2)$$

$$\begin{Bmatrix} x_{II} \\ y_{II} \end{Bmatrix} = \frac{1}{2} \begin{Bmatrix} x_{set3} + x_{set4} \\ y_{set3} + y_{set4} \end{Bmatrix} \quad (3)$$

$$\begin{Bmatrix} x_{CAL} \\ y_{CAL} \end{Bmatrix} = \frac{1}{2} \begin{Bmatrix} x_I + x_{II} \\ y_I + y_{II} \end{Bmatrix} \quad (4)$$

$$\begin{Bmatrix} x_{NOM} \\ y_{NOM} \end{Bmatrix} = \frac{1}{2} \begin{Bmatrix} N_{Xoff} - N \\ \frac{FL}{px} tan(\gamma) \end{Bmatrix} \quad (5)$$

with px = 10 μm (pixel size).

The pixel position $\begin{Bmatrix} x_I \\ y_I \end{Bmatrix}$ and $\begin{Bmatrix} x_{II} \\ y_{II} \end{Bmatrix}$ are independently derived from two data sets each. Their differences give an indication how far the results are reproducible. The last two lines in the Tables 2 and 3 give an average ϕ of these differences from all calibrated pixel positions of each channel. For channels MS4, HR5 and ST7 the average difference ϕ exceed the required 0.1 pixel, i.e. the relative locations of these CCD-arrays were not determined with the required accuracy and must be verified by inflight calibration. All CCD-arrays consist of 6000 sensor elements. The HR5 channel is optically combined by the two CCD-arrays HR5A and HR5B, which overlap within a 3000 pixel interval. Both CCD-arrays were calibrated separately. In Table 3, as in practical application, they are treated as one single CCD-array with 9000 sensor elements, consisting of HR5A-pixels 1 to 4500, corresponding to HR5-pixel 1 to 4500 and HR5B-pixels 1501 to 6000, corresponding to HR5-pixel 4501 to 9000.

3 INFLIGHT CALIBRATION

The principle of inflight calibration can be considered as the reverse process of photogrammetric point determination. Both, inflight calibration and point determination are based on photogrammetric bundle adjustment and require image coordinates of homologous points and navigation data. While point determination aims to extract object information using the exact knowledge of the camera geometry, inflight calibration tries to extract information about the camera geometry using exact knowledge of the object. Thus, a substantial amount of very accurate ground control information is required. Most of the MOMS-02 stereo evaluations suffered from a lack of sufficient accurate ground control points (GCP) which are well identifiable in the imagery. This high resolution evaluation can only profit from control information which has an accuracy of 5 m or better.

The geometric MOMS-2P inflight calibration will be realized in cooperation of 3 institutions: The *German Aerospace Research Establishment* (DLR), the *Chair for Photogrammetry and Remote Sensing, Technical University Munich* (LPF/TUM) and the *Institut Cartogràfic de Catalunya* (ICC). For MOMS-2P the LPF/TUM and the ICC also cooperate in a pilot project to map the whole state of Catalonia. Since

	Multispectral Channels								Stereo Channels			
	MS1		MS2		MS3		MS4		ST6		ST7	
N	Δx	Δy	Δx	Δy	Δx	Δy	Δx	Δy	Δx	Δy	Δx	Δy
25	-0.1	-0.7	-0.2	-1.0	-0.3	2.2	-0.4	0.7	-0.1	-7.0	0.0	0.7
225	0.0	-0.6	-0.1	-0.7	-0.2	2.1	-0.2	0.6	-0.1	-6.9	0.0	0.6
425	0.0	-0.6	-0.1	-0.5	-0.2	2.0	-0.1	0.5	0.0	-6.8	0.0	0.5
625	0.0	-0.6	0.0	-0.4	-0.1	1.9	0.0	0.3	0.0	-6.7	0.0	0.4
825	0.0	-0.7	0.0	-0.3	0.0	1.9	0.0	0.2	0.0	-6.7	0.0	0.3
1025	0.0	-0.7	0.0	-0.2	0.0	1.8	0.1	0.1	-0.1	-6.6	0.0	0.2
1225	0.0	-0.7	0.0	-0.1	0.1	1.7	0.1	0.1	0.0	-6.5	0.0	0.2
1425	0.0	-0.7	0.0	0.0	0.1	1.7	0.1	0.0	0.0	-6.5	0.0	0.1
1625	0.0	-0.7	0.1	0.1	0.1	1.6	0.1	-0.1	0.0	-6.4	0.0	0.0
1825	0.1	-0.7	0.1	0.2	0.1	1.5	0.2	-0.2	0.1	-6.4	0.0	-0.1
2025	0.1	-0.7	0.1	0.3	0.1	1.4	0.2	-0.3	0.1	-6.3	0.0	-0.2
2225	0.0	-0.7	0.1	0.3	0.1	1.4	0.2	-0.4	0.1	-6.3	0.0	-0.3
2425	0.0	-0.7	0.1	0.3	0.1	1.4	0.2	-0.5	0.0	-6.2	0.0	-0.3
2625	0.0	-0.7	0.1	0.4	0.2	1.3	0.2	-0.5	0.0	-6.2	0.0	-0.4
2825	0.1	-0.7	0.1	0.5	0.2	1.3	0.2	-0.6	0.0	-6.2	0.0	-0.5
3025	0.1	-0.7	0.0	0.5	0.2	1.2	0.2	-0.7	0.0	-6.2	-0.1	-0.6
3225	0.0	-0.7	0.0	0.5	0.2	1.1	0.2	-0.7	0.0	-6.3	-0.1	-0.6
3425	0.0	-0.6	0.0	0.5	0.2	1.1	0.2	-0.7	0.0	-6.3	-0.1	-0.6
3625	0.0	-0.5	0.0	0.5	0.1	1.1	0.2	-0.8	0.0	-6.3	-0.1	-0.5
3825	0.1	-0.5	0.0	0.5	0.1	1.1	0.2	-0.8	0.0	-6.3	-0.1	-0.5
4025	0.1	-0.5	0.0	0.5	0.0	1.1	0.1	-0.8	0.0	-6.4	-0.1	-0.4
4225	0.1	-0.5	0.0	0.4	0.0	1.0	0.1	-0.9	0.0	-6.5	0.0	-0.3
4425	0.1	-0.4	0.0	0.4	-0.1	1.0	0.1	-0.9	-0.1	-6.6	0.0	-0.2
4625	0.0	-0.3	0.0	0.4	-0.1	0.9	0.0	-0.9	-0.1	-6.6	0.0	-0.1
4825	0.0	-0.3	0.0	0.4	-0.1	0.9	0.0	-0.9	0.0	-6.7	-0.1	0.1
5025	0.0	-0.2	-0.1	0.3	-0.1	0.8	0.0	-0.9	0.0	-6.7	0.0	0.2
5225	-0.1	-0.2	-0.1	0.3	-0.1	0.8	0.0	-1.0	0.0	-6.8	0.0	0.4
5425	-0.2	-0.1	-0.1	0.2	-0.1	0.7	0.0	-1.0	0.0	-7.0	0.0	0.6
5625	-0.3	-0.1	-0.2	0.2	-0.1	0.6	0.0	-1.0	0.0	-7.1	0.0	0.9
ϕ	0.1	0.1	0.1	0.1	0.1	0.0	0.0	0.5	0.0	0.1	0.3	0.2
σ	0.02	0.03	0.03	0.06	0.03	0.02	0.02	0.02	0.03	0.02	0.06	0.08

Table 2: Correction table for multispectral and stereo channels [pixel]

long, the ICC is successfully engaged in Digital Photogrammetry and has built up a large digital data base comprising full coverage of Catalonia with DTM and color DOI in scale 1:25000 (ground pixel size: 2.2 m) and 70% coverage of B/W DOI in scale 1:5000 (ground pixel size: 0.5 m). Thus, the idea was born to try the automated extraction of ground control information from this data base by use of the multi-scale matching (see subsection 3.1). The DTM has been derived from aerial frame camera images of scale 1:22000 and is stored in the database at 15 m grid size. The accuracy is in the range between 0.5 m and 2.0 m. From cooperation between the ICC and the *Servicio Autonomo de Geografia y Cartografia Nacional* of Venezuela, the ICC also disposes of DTM (30 m grid at 6 m accuracy) and DOI in scale 1:25000 (1.8 m ground pixel size) of an about 12 000 km^2 wide area around Caracas. The two test-sites "Catalonia" and "Venezuela" (see Figure 5 and Figure 6) will be imaged at highest priority whenever the actual weather and sun elevation allow for good illumination and cloud-free conditions. It is planned to cover them both from ascending and descending orbit paths in the stereo mode A, combining high resolution nadir and the two off-nadir stereo channels. In addition the test-site Catalonia will be covered in stereo mode D, combining the blue and near infrared nadir and the two off-nadir stereo channels.

High Resolution Channel					
HR5A			HR5B		
N	Δx	Δy	N	Δx	Δy
25	0.1	-0.2	4501	0.3	0.0
225	0.0	-0.3	4700	0.3	-0.1
425	0.0	-0.3	4900	0.3	-0.1
625	-0.1	-0.3	5100	0.3	-0.1
825	0.0	-0.2	5300	0.3	-0.1
1025	0.0	-0.2	5500	0.3	0.0
1225	0.0	-0.2	5700	0.3	0.0
1425	0.0	-0.2	5900	0.3	0.0
1625	0.1	-0.1	6100	0.2	0.0
1825	0.1	-0.1	6300	0.3	0.0
2025	0.1	0.0	6500	0.2	0.0
2225	0.1	0.0	6700	0.2	0.0
2425	0.1	0.0	6900	0.2	-0.1
2625	0.1	0.1	7100	0.3	-0.1
2825	0.1	0.1	7300	0.2	-0.1
3025	0.1	0.1	7500	0.2	-0.2
3225	0.1	0.1	7700	0.2	-0.3
3425	0.1	0.1	7900	0.2	-0.3
3625	0.1	0.2	8100	0.2	-0.3
3825	0.1	0.1	8300	0.2	-0.3
4025	0.1	0.1	8500	0.2	-0.3
4225	0.1	0.1			
4425	0.1	0.1	ϕ	0.4	0.2
4500	0.1	0.1	σ	0.09	0.05

Table 3: Correction table for high resolution channel [pixel]

3.1 Multi-Scale Matching

In essence the principles of the image matching software used here for the multi-scale matching are the same as have been already used extensively for the automated parallax measurements in MOMS-02/D2 imagery. This software package for intensity based image matching has been developed at DLR and described e.g. in [8].

As MOMS (and also other along-track stereo scanner projects) uses a higher resolution for the nadir looking sensor than for the inclined sensors (MOMS-resolution ratio is 1:3, plans for MOMS-03 aim at 1:2) this software has been generalized for multi-scale matching. This extension is described here. The local least squares matching (LLSM) which is the last step in our current matching procedure anyhow estimates a local affinity transformation between the image chips of a stereo pair. This LLSM has been generalized to accept scale parameters different from 1 as input and to do an aggregation of the higher resolution pixels for comparison to the gray values of the lower resolution for the computation of the intensity based observation equations or - if the observation equations should be formed at higher resolution - generates high resolution from low resolution by bilinear interpolation. See Figure 7 for a graphical representation. Ideally, both directions of resolution change should be done by taking the point spread function of the instrument into account or by some sinc function, respectively. But in reality the gray values have substantial noise added (e.g. instrument noise, radiometric calibration insufficiencies). Thus this sophistication does not pay off for our application and we just use averaging and bilinear interpolation. The new procedure was already successfully applied to MOMS-02 imagery of the Andes [9].

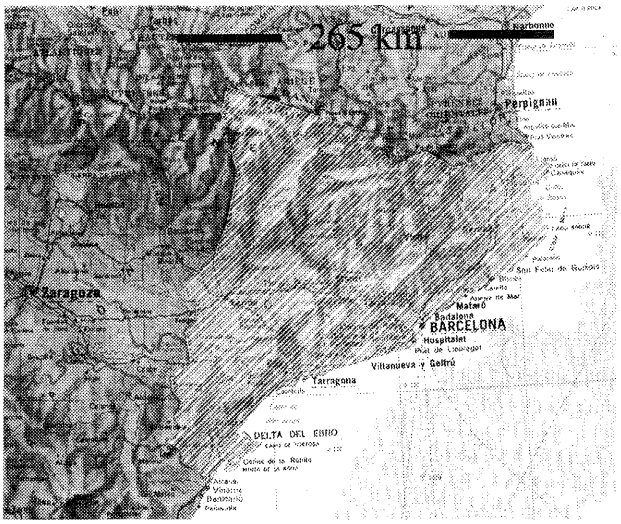

Figure 5: Test-site "Catalonia" (approximately 35 000 km^2)

Figure 6: Test-site "Venezuela" (approximately 12 000 km^2)

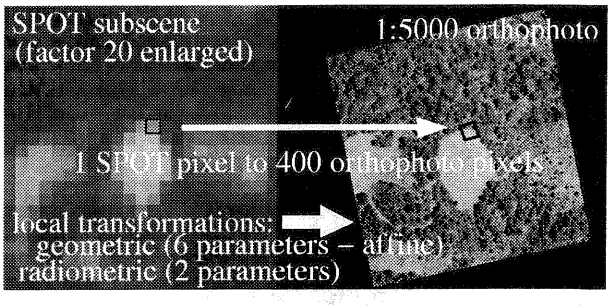

Figure 7: Multi-scale matching principle scheme

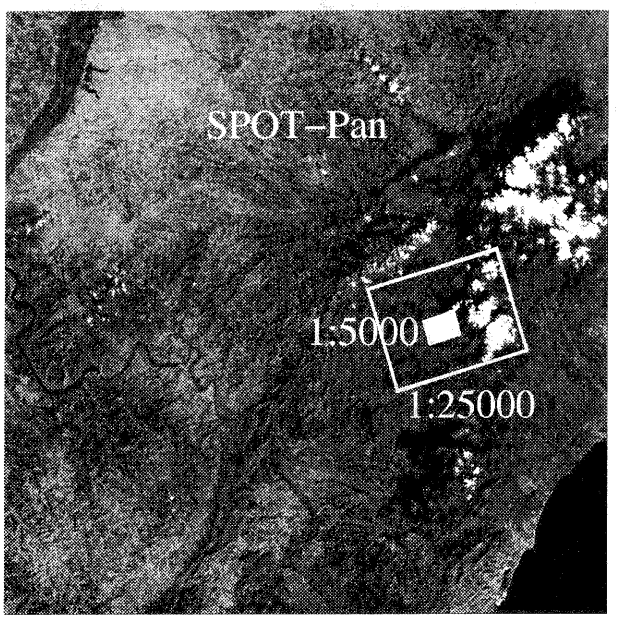

Figure 8: Positions of DOIs in MOMS scene

For a first test the ICC made the following digital data available to DLR:

- one 1:5000 DOI (panchromatic, 7304 columns by 4998 lines)
- one 1:25000 DOI (true color, 6110 columns by 4301 lines, 3 bands) comprising the 1:5000 DOI as a subset
- a SPOT-pan scene (6000 by 6000 pixels, about 10m resolution) comprising the 1:25000 DOI as a sub-scene

Figure 8 shows the SPOT scene and its sub-scenes corresponding to the two DOIs. All scenes have been left radiometrically untouched besides the color DOI from which a panchromatic image was simulated just by averaging the gray values of the color bands for the matching with SPOT-pan.

The procedure for matching these images consists of the following two steps:

1. Matching with very similar resolution (SPOT original with DOIs reduced by factors 4 and 20, respectively) using an image pyramid as described in [8]; the interest operator for the selection of good patterns for image correlation was applied to the SPOT sub-scene.
2. LLSM at different scales by using the results of the low resolution matching as initial values after multiplication of the DOI coordinates with the respective resolution factors 4 and 20; to get standard deviations for the resulting DOI coordinates the LLSM was applied with 3 different chip sizes.

In the case of the 1:5000 DOI the chip sizes used for SPOT were 9^2, 10^2 and 11^2 and, correspondingly, 180^2, 200^2 and 220^2 for the DOI. In the case of the 1:25000 DOI the chip sizes used for SPOT were 12^2, 13^2 and 14^2 and, correspondingly, 48^2, 52^2 and 56^2 for the DOI.

Of course, the SPOT scene and the DOIs were substantially radiometrically different. The overall maximum of the correlation coefficients between SPOT and both DOIs was 0.64 and the quality figure 0.18 (the latter measures the distinctness and acuteness of the peak in the local matrix of normalized correlation coefficients - defined in [7]). Corresponding values for MOMS along-track stereo imagery are 0.8-0.85 and 0.24. Thus, it is clear that one cannot expect the high percentage of convergence of multi-scale LLSM of more than 80% which has been achieved with the MOMS imagery of the Andes.

The results are shown in Table 4. The resulting positions for individual chips can be seen in Figures 9 and 10.

Computer time requirements were about 40 minutes and 2 minutes for the extraction of the number of points in Table 4 for scales 1:25000 and 1:5000, respectively. Much more time

(about 2 hours) went into the manual preparations like sub-scene selection, etc. but this can be much more automated, too. Taking into account that the sub-scenes represented by

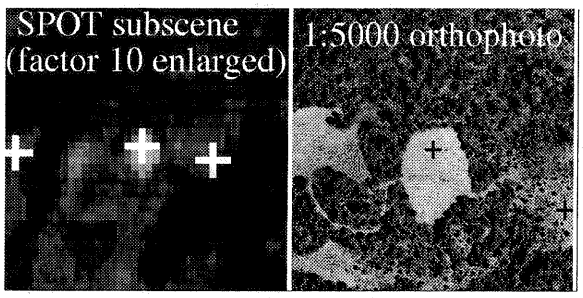

Figure 9: Corresponding image chips of SPOT and 1:5000 DOI

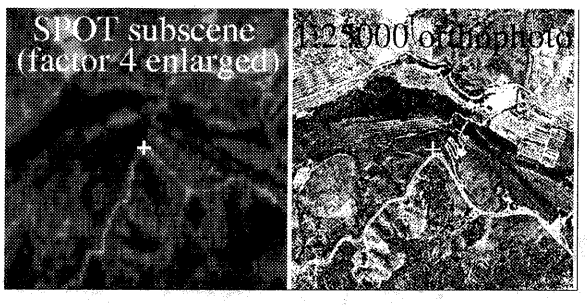

Figure 10: Corresponding image chips of SPOT and 1:25000 DOI

the image chips of the DOIs are very small compared to the full SPOT scene, and that the resolution of the MOMS-2P high resolution nadir looking channel (6m) is even higher than the SPOT resolution this result is very promising as it would lead to much more than the 1000 points which are taken for the simulation study in the next chapter. Of course, DOIs are not error-free but we can certainly hope for an overall ground control accuracy of better than 5m. This value has been introduced in the simulation study which is described below.

type of matching	number of points		standard deviation
	1:5000	1:25000	
1: equal resolution	33	180	$\sim$ 1/3 pixel
2: different resolution	8	35	about 2 m 4 and 0.9 pixel

Table 4: Number and accuracy of automatically found ground control points for the two types of matching

3.2 Simulation (Bundle Adjustment)

In the past a series of simulations was carried out for MOMS-02/D2 to analyze the effect of certain parameters on the accuracy of point determination (e.g. [2], [3], [4]). The simulations are based on the principle of photogrammetric bundle adjustment using generated input data, which was derived from a realistic simulation model. Here new simulations are presented, which follow the same principle. They show the influence of orbit- and ground- control information on the accuracy of camera parameters and orientation angles. The functional model of the bundle adjustment is adapted to the geometric specifications of MOMS and described in [4].

View direction of the lens	forward	nadir	backward
focal length (FL) [mm]	237.2	220.0	237.2
pixel size [μm]	10.0	10.0	10.0
stereo angle γ	-21.9°	0.0°	21.9°
orbit height [km]	400		
swath width [km]	50		
strip length [km]	480		
orbit inclination	51.6°		
intersection angle	68.0°		

Table 5: Fixed simulation parameters

Simulation Model: The parameters used to generate the simulation data are listed in Table 5 and match the nominal values of the MOMS-2P/PRIRODA mission to a large extend. The temporal course of the exterior orientation parameters is modeled by a 3rd order Lagrange polynomial employing orientation images at 4940 lines distance. The functional model of the interior orientation is restricted to 12 parameters by two simplifications: 1.) A common projection center for all three image coordinate systems is used and 2.) the image coordinate system of the HR-lens equals the camera fixed reference coordinate system. Furthermore, equal ground pixel sizes for all three stereo channels were assumed, implying a subsampling of the HR-imagery by factor 3. The FL of the HR-channel therefore was set to 220 mm. The 12 camera parameters are subdivided in 4 parameters for each of the three stereo channels:

- the focal length FL,
- the two-dimensional displacement Δx, Δy and
- the rotation $\Delta\kappa$ of the CCD-array in the image plane.

The simulation is restricted to imaging mode A, resulting in a swath width of 50 km. The intersection angle between ascending and descending orbit paths is 68° at 41.5° average latitude of the test-site Catalonia. The ground control points (GCP) used in the simulations were assumed to be equally distributed and have an accuracy of 5 m in X and Y, and 3 m in Z. The attitude and position of the camera during the time of data recording were assumed to have a relative accuracy of 10" and 5 m, respectively. Altogether, 36 simulation runs were performed in order to investigate the influence of the following 3 parameters on the resulting theoretical standard deviation $\hat{\sigma}$ of the camera parameters and orientation angles (see Table 6): Three different cases were distinguished:

Number of GCP:	100,	500, 1000
Abs. acc. of camera positions:	5 m,	10 m, 20 m
Number of image strips:	1 strip,	2 crossing strips

Table 6: Varied simulation parameters

Case A: Simultaneous determination of the 3 orientation angles $d\varphi_o$ (pitch), $d\omega_o$ (roll), $d\kappa_o$ (yaw), the displacements Δx, Δy and the rotation $\Delta\kappa$ of the two stereo CCD-arrays ST6/ST7 as well as all three focal lengths FL. (Δx, Δy and $\Delta\kappa$ of HR-channel fixed)

Case B: Simultaneous determination of $d\varphi_o$, $d\omega_o$, $d\kappa_o$, Δx, Δy, $\Delta\kappa$ and FL of ST6/ST7 only.
(FL, Δx, Δy and $\Delta\kappa$ of HR-channel fixed)

Case C: Determination of $d\varphi_o$, $d\omega_o$, $d\kappa_o$ only.
(All camera parameter fixed)

Results: The Tables 7 - 11 contain the theoretical standard deviations $\hat{\sigma}$ of the above mentioned unknown parameters, which are deduced from the inverted normal equation matrix and the à posteriori estimate of the reference variance $\hat{\sigma}_o^2$. Since the simulations are performed with generated error-free observations, the à priori σ_o^2 is used instead of $\hat{\sigma}_o^2$; i.e. the resulting theoretical standard deviations $\hat{\sigma}$ are valid for the à priori assumed precision of the observations. The a priori σ_o is chosen as equal to the standard deviations of the image coordinates, which is 0.3 pixel in all computation runs.

In the Tables the following abbreviations were used:

Version aaaa/bb:	aaaa = number of GCP bb = absolute accuracy of the camera positions [m]
FL-HR:	$\hat{\sigma}$ of focal length of the HR5 lens
FL-ST:	$\hat{\sigma}$ of focal length of the ST6/ST7 lenses
Δx, Δy:	$\hat{\sigma}$ of the sensor displacements in the image plane
$\Delta\kappa$:	$\hat{\sigma}$ of the sensor rotation in the image plane
$d\varphi_o$, $d\omega_o$, $d\kappa_o$:	$\hat{\sigma}$ of the 3 orientation angles
[pel]:	[pixel]

The results for case A are shown in the Tables 7 (single strip) and 8 (two crossing strips): The dependency of the theoretical standard deviations on the different versions can be distinguished in 3 groups: The first group consists of FL and $\Delta\kappa$, which are dependent on both, the number of GCP and the absolute accuracy of the camera positions. Δx, $d\varphi_o$ and $d\omega_o$ solely depend on the camera position accuracy, while Δy and $\Delta\kappa$ only depends on the number of GCP. The simultaneous adjustment of two crossing strips improves the results significantly, especially in case of poor control information. It is evident, that even with 10 m absolute camera position accuracy better results are achieved compared to the 5 m single strip versions. This fact might become important, since 5 m orbit accuracy can only be obtained for long data takes of at least 4 minutes time of data recording. If the expected 1000 GCP and 5 m absolute camera position accuracy are available sufficiently precise results are obtained. The focal lengths of all three lenses can be determined with up to 3 μm, the sensor displacement with up to 0.1 pixel, the sensor rotation with up to 2.4" and the rotation angles with up to 7" accuracy. In case B the focal lengths of the ST6/ST7 lenses are determined relative to the focal length of the HR5 lens, which is assumed to be precisely known and fixed. Tables 9 (single strip) and 10 (two crossing strips) show that FL-ST is determined essentially better compared to case A. Concerning the other parameters, there is no significant difference to case A. The 500 GCP versions therefore were omitted. As in case A, two crossing strips lead to essentially improved results. Here even poor control information suffices to determine the sensor displacements with 0.1 pixel accuracy. Dependent on the camera position accuracy FL-ST is determined with standard deviations up to 2 μm. In case C all camera parameters are fixed, assuming perfect à priori knowledge of the camera geometry. Here the control information contributes to the determination of the orientation angles only. Table 11 shows

Version	FL-HR [μm]	FL-ST [μm]	Δx [pel]	Δy [pel]	$\Delta\kappa$ ["]	$d\varphi_o$ ["]	$d\omega_o$ ["]	$d\kappa_o$ ["]
100/20	14.2	14.7	0.4	0.4	8.0	12.4	12.4	11.5
100/10	10.7	11.5	0.2	0.4	7.4	9.1	9.1	11.5
100/5	9.4	10.2	0.1	0.4	7.1	7.4	7.4	11.5
500/20	11.8	12.0	0.4	0.2	5.2	12.4	12.3	8.0
500/10	7.2	7.6	0.2	0.2	4.2	9.0	9.1	8.0
500/5	5.0	5.5	0.1	0.2	3.8	7.3	7.4	8.0
1000/20	11.4	11.6	0.4	0.1	4.8	12.4	12.3	7.4
1000/10	6.6	6.9	0.2	0.1	3.5	9.0	9.1	7.4
1000/5	4.2	4.5	0.1	0.1	3.0	7.3	7.3	7.4

Table 7: Case A: Standard deviations for single strip

Version	FL-HR [μm]	FL-ST [μm]	Δx [pel]	Δy [pel]	$\Delta\kappa$ ["]	$d\varphi_o$ ["]	$d\omega_o$ ["]	$d\kappa_o$ ["]
100/20	8.3	8.5	0.3	0.1	4.9	10.1	11.3	7.9
100/10	4.9	5.1	0.1	0.1	4.3	7.9	8.5	7.9
100/5	3.6	3.8	0.1	0.1	4.2	7.2	7.4	7.9
500/20	8.2	8.3	0.3	0.1	3.8	10.0	10.9	7.3
500/10	4.6	4.7	0.1	0.1	3.1	7.8	8.4	7.3
500/5	3.1	3.4	0.1	0.1	2.8	7.1	7.3	7.3
1000/20	8.1	8.2	0.2	0.1	3.5	10.0	10.7	7.1
1000/10	4.5	4.6	0.1	0.1	2.7	7.8	8.3	7.1
1000/5	2.9	3.2	0.1	0.1	2.4	7.1	7.3	7.1

Table 8: Case A: Standard deviations for two crossing strips

Version	FL-ST [μm]	Δx [pel]	Δy [pel]	$\Delta\kappa$ ["]	$d\varphi_o$ ["]	$d\omega_o$ ["]	$d\kappa_o$ ["]
100/20	4.8	0.3	0.4	8.0	12.4	12.4	11.5
100/10	3.6	0.2	0.4	7.4	9.1	9.1	11.5
100/5	2.7	0.1	0.4	7.1	7.4	7.4	11.5
1000/20	4.6	0.2	0.1	4.8	12.4	12.3	7.4
1000/10	3.2	0.1	0.1	3.5	9.0	9.1	7.4
1000/5	2.4	0.1	0.1	3.0	7.3	7.3	7.4

Table 9: Case B: Standard deviations for single strip

Version	FL-ST [μm]	Δx [pel]	Δy [pel]	$\Delta\kappa$ ["]	$d\varphi_o$ ["]	$d\omega_o$ ["]	$d\kappa_o$ ["]
100/20	3.3	0.1	0.1	4.9	10.1	11.3	8.0
100/10	2.2	0.1	0.1	4.3	7.9	8.5	8.0
100/5	1.9	0.1	0.1	4.2	7.2	7.4	8.0
1000/20	3.3	0.1	0.1	3.5	10.0	10.7	7.1
1000/10	2.2	0.1	0.1	2.7	7.8	8.3	7.1
1000/5	1.8	0.1	0.1	2.4	7.1	7.3	7.1

Table 10: Case B: Standard deviations for two crossing strips

some improvement compared to case A and case B. For the best case, however, the accuracy is still about 7" for all three angles, which nearly is also reached in case A and case B under the same conditions. Summarizing it can be stated,

	1 strip			2 strips		
Version	$d\varphi_0$	$d\omega_0$	$d\kappa_0$	$d\varphi_0$	$d\omega_0$	$d\kappa_0$
100/20	7.1	11.3	6.9	7.2	9.0	6.8
100/5	7.0	7.4	6.9	7.1	7.2	6.8
1000/20	6.9	8.5	6.7	7.1	8.0	6.7
1000/5	6.9	7.2	6.7	7.0	7.1	6.7

Table 11: Case C: Standard deviations ["] for single strip and two crossing strips

that the results of the simulation study are very promising and show, that the accuracy requirements for the geometric calibration can be met also by inflight methods, if control information is available with the expected accuracy. If two, or more, crossing strips are simultaneously evaluated, the requirements on the accuracy of control information can even be relaxed. Since sensor displacements of 0.1 pixel seem to be detectable, changes of the camera geometry, caused e.g. by thermal effects, can be determined and later be considered in the photogrammetric processing of the MOMS-2P imagery.

4 CONCLUSION

The geometric calibration of the stereoscopic CCD linescanner MOMS-2P is subdivided into a laboratory calibration and an inflight calibration part. In the lab-calibration the positions of about 15 pixels per CCD-array were determined with an accuracy better than 0.1 pixel. From the calibration data also locations of the single CCD-arrays relative to a reference coordinate system were computed. They were derived twice from independent measurements. In some channels these two values showed systematic differences up to 0.5 pixels, i.e. the determination of the relative location is not reproducible with the required 0.1 pixel accuracy. Thus it can be concluded, that by lab-calibration the shape of the single CCD-arrays could be determined with sufficient high accuracy, their relative locations, however, still need to be verified by inflight calibration.

The principle of inflight calibration is based on photogrammetric bundle adjustment using a high amount of very accurate ground control information. It could be shown, that the automated GCP extraction by multi-scale matching of linescanner imagery and digital orthoimages is feasible. A first test using SPOT imagery and orthoimages in scale 1:5000 and 1:25000 demonstrated, that more than 1000 GCP with an accuracy better than 5 m can automatically be provided for the inflight calibration.

The simulation study showed, that the inflight calibration of the camera parameters and the orientation angles is possible and the accuracy requirements for the geometric calibration can be met. With the expected 1000 GCP and 5 m absolute accuracy of the camera position, the focal lengths of all three lenses can be determined with up to 3 μm, the sensor displacement with up to 0.1 pixel, the sensor rotation with up to 2.4" and the rotation angles with up to 7" accuracy. If two, or more, crossing strips are simultaneously evaluated, the requirements on the accuracy of control information can even be relaxed.

In order to analyze the impact of temporal and thermal influences on the camera geometry, the inflight calibration is to perform as often as possible during the commissioning phase and should later be repeated in a reasonable time interval on a routine basis.

REFERENCES

[1] E. Dorrer, W. Maier, V. Uffenkamp: "Analytical kinematic sensor orientation of MOMS-02 linear array stereo imagery", *Integrated Sensor Orientation*, Colomina I., Navarro J. (Eds.), pp. 261-273, Wichmann Verlag, Karlsruhe, 1995.

[2] H. Ebner, W. Kornus, G. Strunz, O. Hofmann, F. Müller: "A simulation study on point determination using MOMS-02/D2 imagery", *Photogrammetric Engineering & Remote Sensing*, Vol.57, No. 10, pp. 1315-1320, October 1991.

[3] H. Ebner, W. Kornus: "Point determination using MOMS-02/D2 imagery", *Conference Proceeding IGARSS*, Vol. III, pp. 1743-1746, Helsinki, Finland, 1991.

[4] H. Ebner, W. Kornus, T. Ohlhof: "A simulation study on point determination for the MOMS-02/D2 space project using an extended functional model", *Int. Archives of Photogrammetry and Remote Sensing*, (29) B4, pp. 458-464, Washington D.C., USA, 1992.

[5] C. Fraser, D. Fritsch, P. Collier, J. Shao: "Ground point determination using MOMS-02 earth observation imagery", *Proceedings of the 37th Australian Surveyors Congress*, Perth, Australia, April 13-19, 1996.

[6] W. Kornus, H. Ebner, C. Heipke: "Photogrammetric point determination using MOMS-02/D2 imagery", *Proceedings of SPIE Conference on Remote Sensing and Reconstruction for 3-D Objects and Scenes*, pp. 115-125, San Diego, USA, 9./10. 7. 1995.

[7] M. Lehner: "Triple stereoscopic imagery simulation and digital image correlation for MEOSS project", *Proceedings of ISPRS Commission I Symposium*, pp. 477-484, Stuttgart, 1986.

[8] M. Lehner, W. Kornus: "The photogrammetric evaluation of MOMS-02/D2 mode 3 data (Mexico, Ethiopia)", *Proceedings of SPIE Conference on Remote Sensing and Reconstruction for 3-D Objects and Scenes*, pp. 102-114 San Diego, USA, 9./10. 7. 1995.

[9] M. Lehner, W. Kornus: "Digital photogrammetric processing of MOMS-02/D2 imagery", *ISPRS Congress - Commission III / WG 2*, accepted as poster, July 9-19, 1996.

[10] J. Schiewe, Y. Wang: "MOMS-02/D2 data for the generation and revision of cartographical databases", *Proceedings of MOMS-Symposium*, Cologne, Germany, July 5-7, 1995.

[11] P. Seige: "MOMS: A contribution to high resolution multispectral and stereoscopic earth observation from space", *Photogrammetric Week '93*, Fritsch D., Hobbie D. (Eds.), pp. 109-120, Wichmann Verlag, Karlsruhe, 1993.